The kinematic and spatial deployment of compact, isolated high-velocity clouds

Braun, R.; Burton, W.B.

Astron. Astrophys. 341, 437–450 (1999)

ASTRONOMY
AND
ASTROPHYSICS

The kinematic and spatial deployment of compact, isolated high-velocity clouds

R. Braun[1] **and W.B. Burton**[2]

[1] Netherlands Foundation for Research in Astronomy, P.O. Box 2, 7990 AA Dwingeloo, The Netherlands
[2] Sterrewacht Leiden, P.O. Box 9513, 2300 RA Leiden, The Netherlands

Received 23 July 1998 / Accepted 2 October 1998

Abstract. We have identified a class of high–velocity clouds which are compact and apparently isolated. The clouds are compact in that they have angular sizes less than 2 degrees FWHM. They are isolated in that they are separated from neighboring emission by expanses where no emission is seen to the detection limit of the available data. Candidates for inclusion in this class were extracted from the Leiden/Dwingeloo H I survey of Hartmann & Burton (1997) and from the Wakker & van Woerden (1991) catalogue of high–velocity clouds identified in the surveys of Hulsbosch & Wakker (1988) and of Bajaja et al. (1985). The candidates were subject to independent confirmation using either the 25–meter telescope in Dwingeloo or the 140–foot telescope in Green Bank. We argue that the resulting list, even if incomplete, is sufficiently representative of the ensemble of compact, isolated HVCs – CHVCs – that the characteristics of their disposition on the sky, and of their kinematics, are revealing of some physical aspects of the class. The sample is more likely to be representative of a single phenomenon than would a sample which included the major HVC complexes. We consider the deployment of the ensemble of CHVCs in terms used by others to ascertain membership in the Local Group, and show that the positional and kinematic characteristics of the compact HVCs are similar in many regards to those of the Local Group galaxies. The velocity dispersion of the ensemble is minimized in a reference frame consistent with the Local Group Standard of Rest. The CHVCs have a mean infall velocity of 100 km s^{-1} in the Local Group reference frame. These properties are strongly suggestive of a population which has as yet had little interaction with the more massive Local Group members. At a typical distance of about 1 Mpc these objects would have sizes of about 15 kpc and gas masses, M_{HI}, of a few times 10^7 $M_\odot$, corresponding to those of (sub-)dwarf galaxies.

Key words: ISM: clouds – Galaxy: kinematics and dynamics – galaxies: Local Group – radio lines: ISM

1. Introduction

The term High Velocity Cloud (HVC) has traditionally been assigned to features detected in the λ21 cm line of neutral hydrogen emission which (1) have a radial velocity which is discrepant from that due to Galactic rotation in the direction of the feature (Muller et al. 1963) and (2) subsequently prove to have no obvious stellar counterpart. Aberrant velocity H I features which do have a detected stellar counterpart are, of course, classified as galaxies. It is obvious that this empirical definition of an HVC is not altogether satisfactory, but it underlines the fact that despite some 35 years of study, no generally accepted explanation for the origin, the distance and hence the basic properties of these enigmatic features has yet emerged. The class is effectively defined by *what they are not*. These are features which are *not* related in a simple way to the bulk of Galactic H I via spatial or kinematic continuity and for which we are *not yet aware* of an associated stellar or gaseous component. This last point in particular is one that has by no means been addressed exhaustively and may well prove to be a fruitful avenue for future study. Indeed, recent efforts to detect associated diffuse ionized gas in Hα emission are beginning to meet with some success (Reynolds et al. 1998).

It must be stressed that the term HVC encompasses a fairly wide range of observational phenomena. The distinct system of H I features known as the Magellanic Stream was first recognized by Mathewson, Cleary & Murray (1974) to represent tidal debris originating in the gravitational interaction of the Galaxy with both the Large and Small Magellanic Clouds. This system subtends an extremely large solid angle, defining a belt that encircles the entire Galaxy. Given the spatial deployment and kinematic continuity of this system it can be plausibly assigned a distance of some tens of kpc. Some of the well-studied HVC complexes (known as A, C, H and M) are also distributed over large regions of some tens of square degrees. The distances of two of these complexes have been constrained by absorption–line observations: Danly et al. (1993) determined Complex M to lie within the distance range $1.7 < d < 5$ kpc, and van Woerden et al. (1998) found Complex A to lie within the range $4 < d < 10$ kpc. These absorption–line observations, toward isolated lines of sight in two HVC complexes, are the only direct measures of HVC distances available. At the other extreme, is a class of object that appears to be intrinsically compact, with angular dimensions of a few degrees at most. These objects have no obvious relation either spatially or in velocity with the extended complexes and include the most extreme LSR velocities.

Send offprint requests to: R. Braun or W.B. Burton

It is this last category of compact, peculiar velocity H I emission features which we consider here. The lack of obvious association with either the Galaxy or the large HVC complexes and their similar angular size may allow definition of a single class of HVCs, whose members plausibly originated under common circumstances and share a common subsequent evolutionary history. By utilizing the Leiden/Dwingeloo Survey of H I emission of Hartmann & Burton (1997) and the HVC catalog of Wakker & van Woerden (1991) we have compiled a list of candidate sources. Confirming observations were obtained of all candidates. A representative sample of 66 compact, isolated HVCs (or CHVCs) has emerged, including 23 sources cataloged here for the first time. The sample is distributed quite uniformly over the sky, and yet defines a well-organized kinematic system. The kinematic signature of this system suggests a strongly in-falling population associated with the Local Group gravitational potential. At a typical distance of 1 Mpc they have the dimensions (15 kpc) and gas masses ($M_{HI} \sim 10^{7.5} M_\odot$) of (sub-)dwarf galaxies. A similar suggestion was made by Blitz et al. (1998) based on a more heterogeneous sample of HVCs.

Our discussion is organized as follows. We begin by describing the method of sample selection in Sect. 2, proceed with a description of the newly acquired observations in Sect. 3 and continue with a presentation and discussion of our results in Sects. 4 and 5.

2. Sample selection

The Leiden/Dwingeloo Survey (hereafter abbreviated as the LDS, Hartmann and Burton 1997) of H I emission in the Northern sky above declination about $-30°$ has made it possible to select a well-defined sample of candidate sources of small angular size. This survey provides nearly uniform spatial sampling on a $0\overset{\circ}{.}5$ grid at a sensitivity of about T_B = 0.07 K rms at a velocity resolution of 1 km s^{-1} over the V_{LSR} range of -450 to $+400$ km s^{-1}. When smoothed to the typical HVC velocity width of 20 km s^{-1}, the LDS sensitivity is about 0.02 K rms. The earlier HVC survey of Hulsbosch & Wakker (1988) already provided spatial sampling on a 1° grid above $-17°$ declination with an rms sensitivity of about T_B = 0.01 K rms at a velocity resolution of 16.5 km s^{-1} over the V_{LSR} range of -950 to $+800$ km s^{-1}. The southern sky coverage of Hulsbosch & Wakker was supplemented with data taken on a 2°grid at about half the sensitivity by Bajaja et al. 1985. A catalog based on these two HVC databases was presented by Wakker & van Woerden (1991, hereafter WW91). Since both of the northern surveys were carried out with the Dwingeloo 25 m telescope, with a beam size of about 35 arcmin, neither is Nyquist sampled, but no sources should slip completely through the cracks of the LDS sampling.

An issue of particular concern in a single-coverage survey with a total power instrument, is that of the effect of intermittent radio frequency interference (RFI) on the results. As noted by Hartmann (1994), RFI is often of the form of extremely narrow-band signals which are easily recognized as artificial when seen in a moderately high-resolution spectrum. However, some types of intermittent emission of unknown origin are characterized by a broad spectral signature which is impossible to distinguish from a naturally occurring spectral line profile. Only repeated total-power or interferometric observations can be used to distinguish such broad events from naturally ocurring ones.

We have searched the LDS database for all compact, isolated H I emission features. The method used to identify candidates was to construct a series of "channel maps" of H I emission, each integrated over a velocity interval of 32 km s^{-1} and spanning the entire spatial coverage of the survey ($\delta > -30°$). Compact features (less than 2° FWHM) were cataloged which were spatially and kinematically distinct from Galactic H I emission. The condition of kinematic distinction from the Galaxy corresponds approximately to deviation velocities, as defined by Wakker (1991), of about 50 km s^{-1} or greater. A total of 123 candidates was then subject to new, confirming observation as described in Sect. 3, either using the Dwingeloo 25–meter telescope or, for the weaker of the candidates, the 140–foot telescope of the NRAO in Green Bank.

The 44 candidates whose reality was confirmed in the new data entered the tabulation of CHVCs. Some of the candidates on the initial list extracted from the Leiden/Dwingeloo survey could not be confirmed. In some cases, the initial candidate was only of marginal signal–to–noise ratio. In other cases the second–epoch Dwingeloo spectra were not of sufficient quality to confirm the feature. We note that the interference environment in Dwingeloo had deteriorated substantially during the period between 1993, when the last observations for the LDS were made, and late 1997 and early 1998 when the confirmations were attempted. However, a number of the candidate sources turned out to correspond to cases of non-repeatable broad-band interference. Many of the sources which we could confirm were subsequently imaged with small Nyquist-sampled pointing grids to more accurately determine source positions and sizes as described below.

The first step in compiling the list of compact, isolated HVCs was based on inspection of the Leiden/Dwingeloo survey alone, without consulting any earlier material. In a second step, we consulted the catalog of Wakker & van Woerden (1991), extracting from it all entries identified with a value of the parameter $N \leq 3$, i.e. referring to HVC detections based on an observation at a single pointing, or, at most, on 3 spectra and therefore having a surface area of less than about 4 square degrees. This is true of fully 430 of the total of 561 HVCs cataloged in WW91. We extracted LDS spectra at each of these 430 HVC positions. Of these, 59 had no data in the LDS, since they were below the $-30°$ southern declination limit, 94 could not be confirmed to the sensitivity of the LDS, 62 had a marginal confirmation and 216 could be confirmed with some confidence. Subsequently, we produced images of integrated HI emission at the position of each of the 216 confirmed WW91 sources integrated over a velocity range of 100 km s^{-1} centered on the cataloged velocity centroid. Although all of these sources represent real H I emission features at a peculiar velocity, most of them appear to represent substructure of more extensive HVC complexes. We have extracted only those sources which could be classified as both compact and isolated by demanding: (1) that the half

power contour of each source in our images of integrated H I emission had an area of less than 4 square degrees and (2) that to the sensitivity limit of the LDS the source was not connected to a diffuse emission complex. Only 42 of the 216 confirmed WW91 sources could satisfy those criteria and only 22 of these had not already been included in our sample.

In a final step, we consulted other publications which had reported HVCs which met our criteria of compactness and isolation, but found that these few sources, referenced in column 13 of the table, had already been recovered during the first two steps. We note in this regard that Davies's (1970) cloud, HVC 120−20−444, was excluded by our isolation criterion – it is less than 1° removed from intense emission from M31 – whereas we have no reason to think that this cloud does not show the same intrinsic properties characteristic of the CHVC objects in our tabulation.

3. Data

Observations were obtained with the Dwingeloo 25 m telescope in the periods 1997 September 17 to 19, 1997 November 27 to December 15 and 1998 March 2 to 3, for a total of about 21 days. A variety of switching methods, central frequencies, and total bandwidths was employed in an attempt to optimize baseline quality and avoid locally generated narrow band interference. The most successful strategy employed position switching to a nearby reference position and a total bandwidth of 10 MHz centered within a few hundred km s^{-1} of the Local Standard of Rest. The correlator provided 1024 spectral channels across the band. The single-polarization receiver had a typical system temperature of 35 K. Spectra were calibrated in amplitude with regular observations of the standard region S8, at (l, b)=(207.°0, −15.°0), for which a peak line brightness of T_B = 71 K and line integral of 840 K km s^{-1} over the V_{LSR} interval -5 to $+22$ km s^{-1}was assumed (Williams 1973, Hartmann 1994).

Candidate source positions were initially observed with a single pair of on-source and off-source pointings separated by two degrees in galactic latitude. The typical on-source integration time was 6 minutes, providing an rms sensitivity of about 0.04 K at a velocity resolution of 2 km s^{-1} in the calibrated spectra. As time permitted, confirmed sources were reobserved with a 3×3 grid with a pointing separation of 15 arcmin and subsequently with an additional 3×3 grid with a 30 arcmin pointing separation.

Additional observations were made with the Green Bank 140–foot telescope of the NRAO in 1997 September and 1997 December. A total bandwidth of 10 MHz was employed centered near the candidate frequency. The correlator provided 512 spectral channels in each of two polarizations. The typical system temperature was 20 K. Calibration spectra were obtained on the standard region S8. The observations were made in frequency switched mode with a 10 MHz switch to higher frequency. Typical on-source integration times were less than about 5 minutes.

4. Results

Our catalog of 66 isolated CHVCs is shown in Table 1. The columns of the table are defined in the following way.

Column 1: Running identifying number in the catalog.

Column 2: The integer rounded Galactic longitude and latitude together with the integer rounded LSR velocity. All three coordinates in the designation are derived from the best available data for each source as outlined below.

Column 3: I/C = Initial/Confirmation data. The initial source of the candidate positions and velocities was either the LDS, indicated by "LD" in this column, or Wakker & van Woerden (1991), indicated as "W". Confirming data were required in all cases to establish the repeatability of the source spectrum. In some cases the LDS provided independent confirmation of the "W" sources, while in other cases new data were obtained with the NRAO 140-foot telescope in Green Bank, denoted with "GB" or the Dwingeloo 25-m telescope, denoted with "D". Those cases where Nyquist sampled maps were made with the Dwingeloo telescope are indicated with the designation "Dm".

Columns 4 and 5: Galactic (l, b) coordinates of the source centroid as determined from the new Nyquist sampled images of the integrated H I where available (designated with a "Dm" in column 3) and otherwise from the integrated H I data of the LDS. Positional accuracy is about 5 arcmin for the "Dm" data and about 15 arcmin for the LDS.

Columns 6 and 7: J2000 right ascension and declination coordinates of the source centroid. Positional accuracy is about 5 arcmin for the "Dm" data and about 15 arcmin for the LDS.

Columns 8 and 9: The radial velocity measured with respect to the Local Standard of Rest and Galactic Standard of Rest. For those members of the ensemble which were subject to detailed mapping, the $v_{\rm LSR}$ refers to the velocity at the centroid position; for the other CHVCs, the velocity is that following from a Gaussian decomposition of the representative spectrum plotted in Fig. 1. The galactic standard of rest is defined by $v_{\rm GSR} = 220\cos(b)\sin(l) + v_{\rm LSR}$.

Columns 10, 11 and 12: The peak brightness temperature of the Gaussian component resulting from decomposition of the representative spectrum plotted in Fig. 1, the FWHM velocity width, and the integrated flux contributed by the component.

Columns 13, 14 and 15: The deconvolved major and minor axis FWHM dimensions and the major axis position angle (East of North) in (l, b) coordinates. These are derived from the new Nyquist-sampled images of the integrated H I where available (designated with a "Dm" in column 3) and otherwise from the integrated H I data of the LDS.

Column 16: References to earlier mentions of the tabulated HVCs, coded as follows: BBWH99, Burton, Braun, Walterbos, & Hoopes 1999; CM79, Cohen & Mirabel 1979; G81, Giovanelli 1981; GH77, Giovanelli & Haynes 1977; H78, Hulsbosch 1978; H92, Henning 1992; M81, Mirabel 1981; MC79, Mirabel & Cohen 1979; W#, Wakker & van Woerden 1991; and Wr79, Wright 1979.

Each of the CHVCs is illustrated in Fig. 1 where the integrated H I intensity from the vicinity of each source is displayed, together with a representative H I spectrum. The images were obtained from an integration over 200 km s^{-1} velocity width

Table 1. Compact, isolated high-velocity clouds.

#	designation HVC $lll \pm bb \pm vvv$	data I/C	l (°)	b (°)	RA (h m)	Dec (° ′)	$v_{\rm LSR}$ (km/s)	$v_{\rm GSR}$ (km/s)	$T_{\rm max}$ (K)	FWHM (km/s)	$\int {\rm T_B} dV$ (K km/s)	Maj (°)	Min (°)	PA (°)	references
1	HVC 017−25−218	LD/Dm	16.58	−25.28	19 59.1	−24 55	−227	−170	0.45	13.5	6.5	0.6	0.2	20	M81
2	HVC 018+47−145	LD/Dm	18.15	+47.01	15 39.7	10 18	−145	−98	0.15	42.8	6.8	1.1	0.5	60	W57
3	HVC 024−02−285	LD/D	24.29	−1.96	18 42.6	−08 35	−284	−194	0.32	25.8	8.7	1.1	0.5	90	
4	HVC 030−51−119	LD/Dm	29.56	−50.69	21 58.3	−22 42	−123	−54	0.67	39.4	28.0	1.1	0.4	95	
5	HVC 031−20−287	LD/D	31.38	−20.09	20 01.0	−10 20	−287	−179	0.42	36.0	15.9	0.8	0.5	40	W386
6	HVC 032−31−299	LD/Dm	31.90	−30.77	20 41.7	−14 18	−309	−209	0.24	31.2	7.9	0.5	0.3	90	W443
7	HVC 039−37−231	LD/Dm	38.72	−37.31	21 15.6	−11 50	−238	−129	0.33	17.7	6.1	0.6	0.2	60	W482
8	HVC 039−33−260	LD/D	38.78	−33.47	21 01.6	−10 08	−260	−145	0.43	26.3	12.1	0.7	0.7	0	W460
9	HVC 039−31−265	LD/Dm	39.40	−30.67	20 52.4	−08 25	−278	−158	0.33	35.9	12.7	1.8	0.7	120	W442
10	HVC 040+01−282	W/LD	40.20	+0.60	19 02.6	06 44	−282	−140	0.12	42.6	5.5	1.0	0.5	90	W289
11	HVC 043−13−302	LD/Dm	42.91	−13.11	19 56.3	02 41	−314	−168	0.53	27.6	15.6	1.0	0.7	30	G81,W348
							−267	−121	0.22	39.7	9.3				
12	HVC 047−52−129	LD/D	47.14	−51.73	22 19.4	−12 52	−129	−29	0.24	25.4	6.4	2.3	2.0	90	W521
13	HVC 050−68−187	LD/Dm	49.80	−68.28	23 23.4	−19 09	−201	−139	0.19	31.3	6.3	0.6	0.4	35	
14	HVC 060−65−206	W/LD	59.80	−64.60	23 18.6	−13 51	−206	−124	0.12	38.3	5.1	0.7	0.5	30	W545
15	HVC 069+04−223	LD/Dm	69.16	+3.75	19 50.1	33 41	−234	29	0.24	34.0	8.8	1.0	0.9	30	
16	HVC 070+51−146	W/LD	70.10	+50.80	15 48.8	43 53	−146	−15	0.20	33.0	7.0	1.2	0.6	60	W44
17	HVC 087+03−289	LD/Dm	86.82	+2.92	20 46.3	47 50	−298	−79	0.16	35.7	6.1	1.5	0.4	110	W278
18	HVC 092−39−367	LD/D	92.47	−39.41	23 14.4	17 39	−367	−197	0.21	27.0	6.0	1.6	1.2	115	
19	HVC 094+08+080	LD/Dm	94.40	+7.93	20 51.7	56 52	+65	+282	~ 0.3	–	–	0.0	0.0	0	BBWH99
20	HVC 095−63−314	W/LD	94.70	−63.20	00 02.1	−03 04	−314	−215	0.35	26.9	10.1	1.0	0.8	160	W542
21	HVC 100−49−383	LD/Dm	99.58	−48.89	23 49.8	11 10	−388	−245	0.21	51.8	11.8	0.8	0.5	45	
22	HVC 107−30−421	LD/GB	107.49	−29.72	23 48.7	31 16	−419	−237	0.18	31.5	6.2	1.2	0.5	50	W437,H92
23	HVC 108−21−388	LD/GB	108.10	−21.42	23 39.6	39 22	−395	−200	0.11	26.1	3.1	0.6	0.4	110	W389
24	HVC 111−07−466	LD/GB	110.58	−7.00	23 27.1	53 50	−466	−262	0.17	24.9	4.6	0.8	0.7	65	H78,CM79,Wr79,W318
25	HVC 114−10−430	LD/GB	113.56	−10.49	23 52.1	51 18	−440	−242	0.77	10.0	8.2	0.4	0.3	90	H78,CM79,W330
26	HVC 115+13−275	LD/Dm	115.39	+13.38	22 56.9	74 33	−260	−67	0.16	95.4	16.5	1.1	0.6	100	
27	HVC 118−58−373	W/LD	118.50	−58.20	00 42.1	04 35	−373	−271	0.66	30.8	21.6	1.0	0.7	140	MC79,G81,W532
28	HVC 119−73−301	W/LD	118.50	−73.10	00 46.2	−10 16	−301	−245	0.13	31.6	4.4	0.7	0.4	80	W555
29	HVC 119−31−381	LD/D	119.17	−30.92	00 36.2	31 50	−381	−216	0.29	24.6	7.5	0.9	0.8	100	Wr79,W444,H92
30	HVC 123−32−324	W/LD	122.90	−32.20	00 51.3	30 40	−324	−168	0.16	32.7	5.4	0.7	0.4	30	W446
31	HVC 125+41−207	W/LD	125.20	+41.40	12 24.0	75 36	−207	−72	2.10	5.9	13.2	1.3	0.7	120	W84
32	HVC 129+15−295	LD/Dm	128.82	+14.97	02 33.2	76 40	−306	−140	0.44	18.1	8.5	0.0	0.0	0	W231
33	HVC 133−76−285	LD/Dm	132.80	−75.87	01 01.3	−13 11	−296	−257	0.16	37.9	6.3	0.6	0.1	90	W557
34	HVC 146−78−275	LD/D	146.01	−77.65	01 11.4	−15 41	−275	−249	0.16	23.9	4.1	0.9	0.9	110	W560
35	HVC 148−32−144	LD/Dm	147.89	−31.92	02 25.7	26 21	−146	−47	0.18	35.2	6.8	0.5	0.3	80	
36	HVC 148−82−258	LD/Dm	148.04	−82.46	01 05.0	−20 16	−267	−252	0.47	20.2	10.1	0.0	0.0	0	
37	HVC 149−38−140	LD/D	149.24	−37.92	02 19.1	20 26	−140	−51	0.27	29.3	8.3	1.0	0.7	100	
38	HVC 157+03−185	LD/D	156.63	+2.73	04 46.4	49 35	−185	−98	0.18	20.3	3.8	1.5	1.1	90	W275
39	HVC 158−39−285	W/LD	157.80	−39.20	02 41.3	16 07	−285	−221	0.16	37.9	6.4	1.3	0.8	150	W486
40	HVC 162+02−170	LD/Dm	161.87	+2.46	05 04.5	45 20	−181	−113	0.59	27.9	17.5	0.8	0.7	55	W277
41	HVC 171−54−229	LD/Dm	170.97	−53.77	02 35.7	00 55	−235	−215	0.49	23.7	12.4	1.0	0.4	80	H78,W525
42	HVC 172+51−114	W/LD	171.60	+51.40	10 00.6	46 18	−114	−94	0.27	38.6	11.0	3.0	1.2	150	W39
43	HVC 173−60−236	W/LD	172.70	−59.50	02 23.1	−05 48	−236	−222	0.22	17.6	4.1	0.7	0.5	90	W536
44	HVC 186+19−114	W/LD	186.20	+18.90	07 16.9	31 46	−114	−136	1.03	20.4	22.4	1.0	0.8	140	W215
45	HVC 191+60+093	LD/GB	190.86	+60.36	10 36.9	34 10	+93	73	0.38	29.6	12.0	1.0	0.9	75	
46	HVC 198−12−103	W/LD	197.70	−11.60	05 41.8	07 54	−103	−169	0.48	23.9	12.2	1.0	0.8	110	W343
47	HVC 200+30+080	LD/Dm	200.22	+29.72	08 22.2	23 20	+75	+9	0.50	28.9	15.3	0.0	0.0	0	
48	HVC 200−16−091	W/LD	200.50	−15.70	05 32.9	03 30	−91	−165	0.56	27.1	16.0	1.1	0.9	150	W362
49	HVC 202+30+057	LD/D	202.23	+30.38	08 27.4	21 55	+57	−15	1.12	26.0	30.9	1.8	1.3	35	
50	HVC 204+30+075	LD/Dm	204.15	+29.80	08 27.5	20 09	+61	−17	1.19	33.9	42.8	0.8	0.6	145	
51	HVC 220−88−265	LD/D	219.75	−88.06	01 00.1	−27 21	−265	−270	0.30	12.8	4.2	1.5	1.3	90	
52	HVC 224−08+192	W/LD	224.20	−8.00	06 43.0	−13 38	+192	+40	0.24	26.3	6.8	1.2	0.9	90	W325
53	HVC 225+36+082	W/LD	224.60	+35.90	09 19.2	06 59	+82	−43	0.22	36.3	8.6	1.3	1.0	80	W115
54	HVC 225−42+190	LD/Dm	224.87	−41.60	04 29.8	−26 08	+184	+68	0.22	35.8	8.2	0.8	0.5	95	
55	HVC 227−34+114	LD/Dm	226.84	−33.57	05 06.0	−25 30	+115	−19	0.60	32.3	20.7	0.8	0.4	90	
56	HVC 229−74−168	LD/Dm	228.93	−74.22	02 02.0	−30 22	−174	−219	0.25	33.4	8.8	0.7	0.5	120	
57	HVC 230+61+165	LD/GB	230.36	+60.62	10 55.2	15 28	+155	+72	0.23	29.3	7.1	1.4	0.7	120	
58	HVC 235−74−150	LD/Dm	235.26	−73.74	02 02.7	−32 10	−157	−208	0.27	23.1	6.6	0.7	0.5	80	
59	HVC 237+50+078	W/LD	236.70	+49.80	10 25.4	06 42	+78	−41	0.19	36.8	7.6	1.2	1.2	0	W47
60	HVC 241+53+089	W/LD	241.00	+53.40	10 43.5	06 41	+89	−26	0.15	59.7	9.8	1.2	0.8	50	W34
61	HVC 263+27+153	W/LD	263.00	+26.90	10 16.6	−23 43	+153	−42	1.10	22.2	26.4	1.3	0.8	40	W162
62	HVC 267+26+216	W/LD	267.30	+26.10	10 28.1	−26 41	+216	+19	2.61	19.0	52.8	1.6	1.0	10	GH77,W176
63	HVC 271+29+181	W/LD	271.50	+28.90	10 48.9	−26 23	+181	−12	0.92	24.1	23.6	1.3	0.8	110	W163
64	HVC 284−84−174	W/LD	284.00	−84.00	01 00.7	−32 47	−174	−196	0.35	28.6	10.5	1.2	1.0	0	W561
65	HVC 340+23−108	LD/D	340.12	+22.51	15 29.6	−28 43	−108	−177	0.36	32.4	12.5	1.2	0.5	90	
66	HVC 358+12−137	LD/D	358.11	+12.29	16 55.6	−23 33	−137	−144	0.56	19.4	11.5	1.1	0.7	120	

of the LDS data (Hartmann & Burton 1997), centered near the mean velocity of the feature. (In a few cases, the relatively small deviation velocity of the feature required a different setting of the velocity interval.) The data are used as they were extracted from the Hartmann & Burton (1997) CD–ROM, i.e. with no additional baseline manipulation. The contours in the images

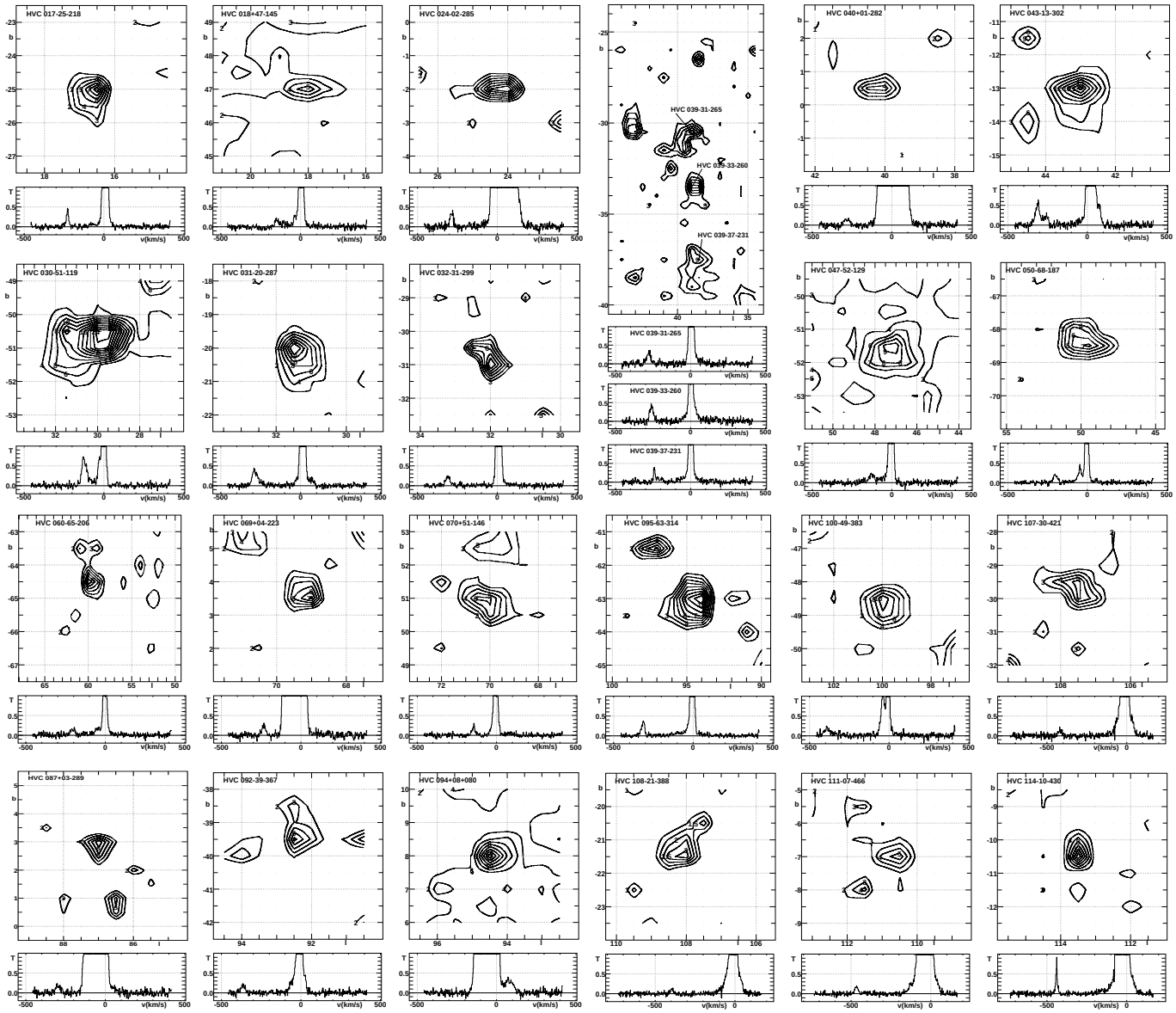

Fig. 1. Images of integrated H I emission, paired with a representative spectrum, for each of the 66 compact, isolated HVCs tabulated in our sample. H I emission is integrated over a velocity extent of 200 km s^{-1}, centered approximately on the mean velocity of the CHVC. The data were extracted from the Leiden/Dwingeloo survey CD–ROM. The associated spectrum refers to the direction in the $0.^\circ5 \times 0.^\circ5$ grid nearest to the peak of the integrated emission. For those compact HVCs confirmed with new Green Bank data (as indicated in column 3 of the table), the spectrum displayed was obtained on the 140–foot telescope; for all other entries, the spectrum displayed is from the Leiden/Dwingeloo survey.

represent integrated intensities labelled in units of K km s^{-1}, which can be converted to column depth in units of H I atoms cm^{-2} by multiplying by 1.8×10^{18}, under the usual assumption of negligible optical depth. The representative spectrum refers to the direction in the $0.^\circ5 \times 0.^\circ5$ grid nearest to the peak of the integrated emission. For those compact HVCs whose reality was confirmed in Green Bank (as indicated in column 3 of the table), the spectrum displayed was obtained on the 140–foot telescope; for all other entries, the spectrum displayed is from the Leiden/Dwingeloo survey after a single pass of Hanning smoothing.

4.1. Comments on a few individual CHVCs

The entries in Table 1 represent a range of profile shapes. The FWHM values, for example, range from 5.9 km s^{-1}, characteristic of a very narrow, cold H I feature in the conventional gaseous disk, to 95.4 km s^{-1}, characteristic of some moderately massive external galaxies. We remark here on some of the individual members of the ensemble. It is an important question, of course, whether the tabulation of compact HVCs represents a single physical phenomenon, or whether it contains interlopers from other classes of objects.

One of the objects listed in the table has, in fact, been revealed as an interloper. The $19^{\rm th}$ entry, designated

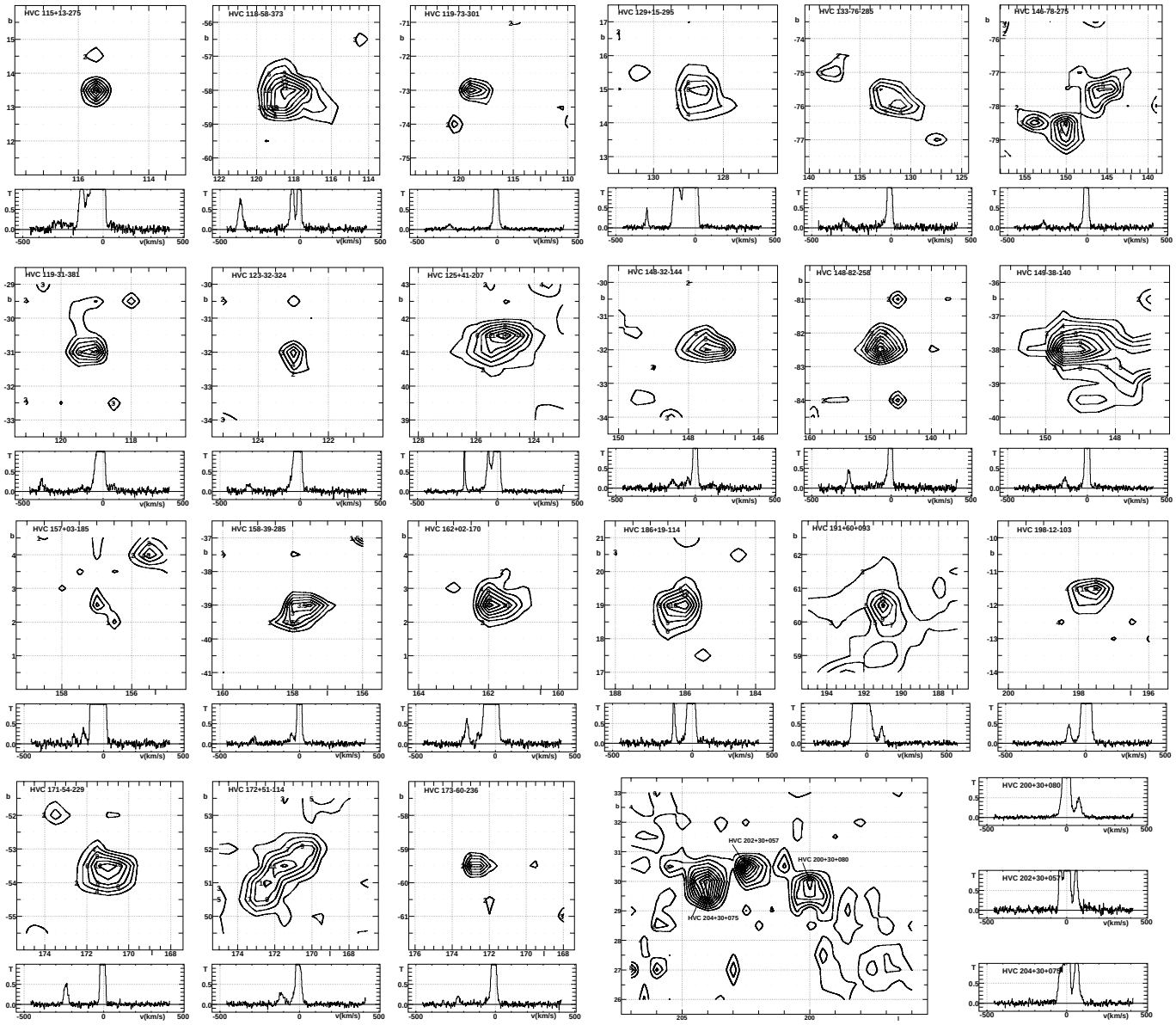

Fig. 1. (continued)

HVC 094+08+080, is a large, nearby, low–surface–brightness galaxy, Cepheus 1, discovered during the course of this investigation. Deep multicolor and spectroscopic optical follow–up observations showed the presence of stars and H II regions, and radio synthesis interferometry confirmed that the galaxy has the optical properties and H I rotation signature of a low–surface–brightness spiral galaxy (Burton et al. 1999). We have retained this object in our tabulation, and in the various plots. It is instructive to see how the H I properties of this interloper galaxy might differ from those of the CHVCs, and how its spatial and kinematic deployment on the sky might resemble that of the ensemble of CHVCs. Warned by the the presence of Cepheus 1 in our compilation, we searched the Digital Sky Survey CD–ROM in the direction of each of the sources listed in the table, but found a clear optical counterpart for no entry other than HVC 094+08+080. We can not rule out that other entries would reveal an optical counterpart in deeper optical data; indeed, very deep optical searches are called for. Even if no further large galaxy lurks in the tabulation, the distinction between CHVCs and dwarf galaxies with very weak star formation remains to be made. We view establishing the nature of such a distinction as an important challenge.

We note a few of the entries individually:

4.1.1. CHVCs with exceptionally broad, or exceptionally narrow, H I lines

Most of the HVC flux studied in earlier investigations is contributed from complexes, or from extended features; these commonly show substantial kinematic gradients consistent with rotation or shearing. The CHVCs considered here, however, are largely subsumed into a single beam; although the kine-

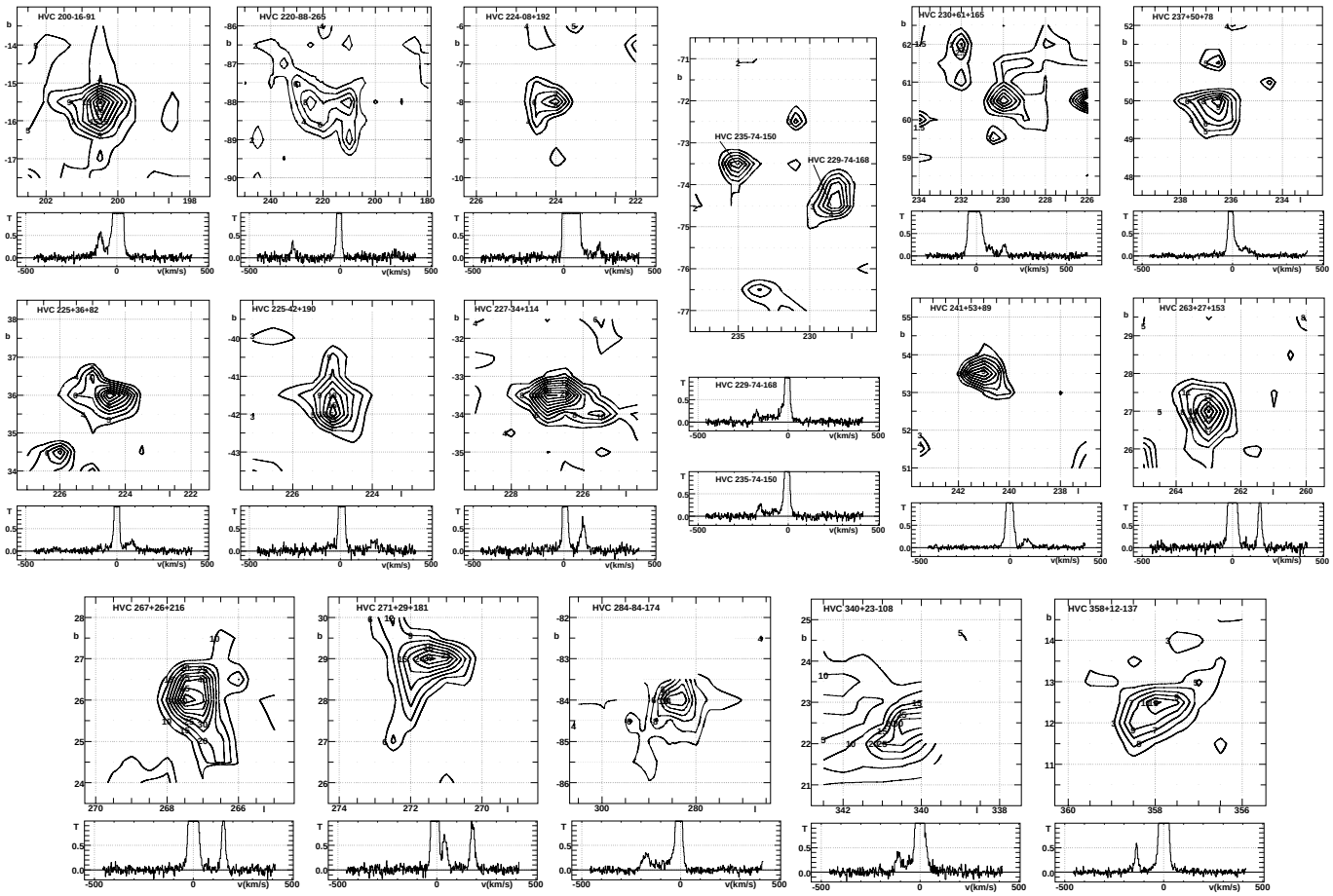

Fig. 1. (continued)

matic information is largely unresolved, kinematic considerations in addition to the systemic velocity remain relevant. HVC 115+13−275 has a FWHM of 95.4 km s^{-1}; the exceptional width of the feature and its location at low b suggests that a deeper optical look than that afforded by the POSS would be appropriate, as would an H I synthesis observation looking for kinematic structure contributed either by rotation of a single entity or by blending of subunits, each moving with a different velocity. HVC 114−10−430 and HVC 125+41−207 have, on the other hand, H I signatures which are exceptionally narrow not only for HVCs, but for any H I emission lines. The line width of HVC 125+41−207, FWHM$= 5.9 \pm 1.6$ km s^{-1}, corresponding to $\sigma_{\rm v} = 2.5 \pm 0.7$ km s^{-1}, is sufficiently small that it may even be used to constrain the kinetic temperature of the gas, $T_{\rm k} < 750$ K. It also constrains the line–of–sight component of any rotation or shear in a single object, as well as the range of kinematics if the object should be an unresolved collection of subunits.

4.1.2. CHVCs near the galactic equator

HVCs located on lines of sight traversing the gaseous disk of the Milky Way display the horizontal component of their space motion. Large horizontal motions are difficult to account for in terms of a galactic fountain model (Shapiro & Field 1976, Bregman 1980). Burton (1997) has noted that HVCs do not contaminate the H I terminal–velocity locus in ways which would be expected if they pervaded the galactic disk, and that this observation constrains HVCs either to be an uncommon component of the Milky Way disk, confined to the immediate vicinity of the Sun, or else to be typically at large distances beyond the Milky Way disk. In our tabulation, HVC 024−02−285, HVC 040+01−282, and HVC 111−07−466 are examples of low $|b|$ CHVCs at velocities unambiguously forbidden in terms of normal galactic rotation. The lines of sight in the directions of each of these features traverse some tens of kpc of the disk before exiting the Milky Way: unless one is prepared to accept these HVCs as boring through the conventional disk (for which there is no evidence), and atypical in view of the cleanliness of the terminal–velocity locus, then their distance is constrained to be large.

4.1.3. CHVCs near the galactic poles

Similarly, HVCs located near the galactic poles offer unambiguous information on the vertical, z, component of their space motion. Burton (1997) noted that the vertical thickness of the galactic H I layer is well measured with a scale height

of $h_z \sim 100$ pc, and so consequently the HVCs either do not commonly populate the lower galactic disk/halo transition region or else the z component dominates the total space motion, which seems unlikely and is contradicted by the examples in the preceding paragraph. Examples of high vertical velocities from our tabulation include HVC 119−73−301, HVC 148−82−258, and HVC 220−88−265. These examples are from the southern galactic hemisphere, with negative velocities. The distribution of z motions over the entries in the tabulation are clearly skewed to negative velocities.

4.1.4. CHVCs in the Milky Way cardinal directions

HVCs in the cardinal directions are interesting because some ambiguities are removed in these special cases. For example, HVC 087+03−289, located in the direction of the solar motion partaking in galactic rotation, has a velocity unambiguously forbidden for any object within the Milky Way. The substantial velocities of HVC 173−60−236, and HVC 358+12−137, located (albeit at substantial latitudes) in directions perpendicular to the vector of galactic rotation, are also unambiguously forbidden.

4.2. Completeness and homogeneity of the sample

It is appropriate to consider what selection effects might play a role in the statistics derived from the material in Table 1. We comment below on the relevance of the observational parameters of sensitivity, velocity coverage, and spatial coverage.

The most stringent of our criteria was the requirement of independent confirmation. The Leiden/Dwingeloo survey does, however, involve so much data that confirming every 5–σ spike would have taken an investment of telescope time which we were not able to make. There are features, even in the integrated H I images shown here, which we have no reason to consider spurious, but which we simply have not yet confirmed: in Fig. 1 examples are seen near $l, b = 86.^\circ5, +1.^\circ0$ in the moment map of HVC 087+03−289; and near $l, b = 43.^\circ0, -30.^\circ0$ in the moment map of HVC 039−31−265; both of these examples of not–yet–confirmed features are unambiguously in the HVC regime, and stem from spectra not observed contiguously. (The observing strategy involved stepping $0.^\circ5$ in l, at a constant b, over a 5° interval of longitude.) We see no reason to expect that these features, and many others, could not be confirmed.

Our use of the terms ‘compact’ and ‘isolated’ is somewhat subjective, as can be gauged by inspection of the integrated H I images. ‘Compact’ is the simpler concept since we have used the somewhat arbitrary definition of a maximum mean angular size (averaged over the major and minor axis of elongated features) of 2° FWHM. The choice of a 2° limit was motivated by what appeared to be a natural break point in the size distribution of HVC features cataloged by WW91. ‘Isolated’ refers, of course, to the sensitivity level of the currently available data. It is not ruled out that some of the features which we tabulate as isolated in (l, b, v) space would be shown under scrutiny of more sensitive data to be embedded in a weaker envelope, or even to be part of a large, but relatively weak, complex or stream. For example, entries 47, 49, and 50 in our table, adjacent on the sky and at comparable velocities, might prove blended under deeper scrutiny.

The well–known HVC complexes show a range of structures, and within a complex there are certainly knots of enhanced emission (see Wakker & Schwarz 1991). We did not accept such knots, and so could plausibly have discriminated against a compact, isolated HVC which happens to lie in projection against an unrelated extended HVC stream.

Although the Leiden/Dwingeloo survey had been corrected for stray radiation (Hartmann et al. 1995), neither the new Dwingeloo nor the new Green Bank data were so corrected. Emission entering the far–sidelobe pattern is largely contributed by H I lying, at relatively modest velocities, in the conventional gaseous disk of the Milky Way: stray–radiation is not expected over most of the HVC velocity regime. Furthermore, stray radiation is contributed from large solid angles, and thus is diffusely distributed, not concentrated into point, or very compact, sources like those entering this discussion. Therefore we view our results as uncontaminated by stray radiation.

Selection of candidate CHVCs from the Leiden/Dwingeloo survey was primarily determined from a significant intensity after smoothing to 32 km s^{-1} velocity resolution, and a lack of blending. On the $0.^\circ5 \times 0.^\circ5$ grid at $\delta \geq -30^\circ$, unblended clouds (i.e. generally those with a deviation velocity greater than 50 km s^{-1}) emitting with a 5–σ peak intensity greater than $T_\mathrm{B} \sim 0.1$ K, and with a FWHM velocity extent broader than 20 km s^{-1}, are unlikely to have been missed. Narrow clouds (< 10 km s^{-1}) weaker than about 0.2 K peak temperature will be underrepresented in the list drawn from the smoothed Leiden/Dwingeloo data. Although the FWHM of most of the CHVCs tabulated here is greater than 20 km s^{-1}, a few are considerable narrower, and it is not unexpected that some faint sources would be missing from our compilation because they were diluted by a coarse channel spacing. An overall completeness level of 0.2 K in peak brightness is indicated.

The total range of the velocity coverage of the Leiden/Dwingeloo survey is conservatively quoted as $-450 < v_\mathrm{LSR} < +400$ km s^{-1}, but in almost all cases it extends usefully ten or more km s^{-1} further on both extremes; the total range of the Wakker & van Woerden material is larger, extending from -900 to $+750$ km s^{-1}. The HVC with the most extreme velocity known is that detected by Hulsbosch (1978), and further observed by Cohen & Mirabel (1979) and by Wright (1979), tabulated here as HVC 111−07−466: its v_LSR is -466 km s^{-1}. Although a few other HVCs are known with velocities less than -400 km s^{-1}, none is known with comparably extreme positive velocities. Therefore it seems reasonable to expect that the tabulation is not incomplete as a consequence of the velocity range of the observational material.

In the second stage of preparing our list of CHVC candidates, we used the Wakker & van Woerden compilation as input. The angular lattice size of that material is larger than that of the Leiden/Dwingeloo survey. At $\delta < -18^\circ$, the angular spacing of the Bajaja et al. (1985) data is $2^\circ \times 2^\circ$. At $\delta > -18^\circ$, the latitude interval of the Hulsbosch & Wakker (1988) data

is 1° throughout, but the longitude interval varies from 1° at $|b| < 45^\circ$ to larger values at larger $|b|$, while maintaining approximately $\Delta l = 1^\circ$ in true–angle spacing. Even though the Leiden/Dwingeloo survey is not fully sampled to the Nyquist level, the $0.^\circ5$ sampling interval with a $36'$ beam renders it unlikely that a compact HVC, at the intensity level being considered here (0.2 K peak brightness temperature), would have escaped notice in that data because of undersampling. On the other hand, a compact HVC in our tabulation could well remain undetected in the Hulsbosch & Wakker and Bajaja et al. data as a consequence of the relatively coarse grid spacing. Hulsbosch & Wakker (1988) estimate that their material is essentially complete for point–source clouds with a central brightness temperature greater than 0.05 K which lie on an observational grid point, but only about 57% complete for point–source clouds with a central brightness temperature of 0.2 K which might not lie on an observational grid point. Insofar as the WW91 $N \leq 3$ sources served as input for subsequent confirmation, there may be some additional incompleteness in the strip between $\delta = -30^\circ$ and -18°, where the Bajaja et al. data represent a coarser ($2^\circ \times 2^\circ$) sampling and a somewhat less sensitive detection limit than that of Hulsbosch & Wakker.

The above considerations indicate why some CHVCs (23 of the 66) were found in the Leiden/Dwingeloo data but not in the data used by Wakker & van Woerden. It is also possible that a weak CHVC, fortuitously located in the relevant parameter space of the observations, would be detected in the Wakker & van Woerden data but not in the Leiden/Dwingeloo. However, any incompleteness due either to sensitivity, or to lattice size, or to velocity increment, would be approximately the same everywhere on the observed sky, and so would not render the tabulation made here unrepresentative of the compact HVCs.

Other selection effects are plausibly more systematic in specific velocity ranges and in location. Because the compilation involved Dwingeloo data in all cases, either for the initial identification or for the confirmation, or for both, material is missing where the sky is not accessible from the Netherlands. The boundary at $\delta \leq -30^\circ$ is indicated by the distorted oval drawn in Fig. 2. In view of what is known about the distribution of high–velocity clouds in the deep southern hemisphere, it seems reasonable to expect that the southern CHVCs which have been missed would likely be predominantly at positive radial velocities. We note that all 6 of the Local Group galaxies known in the zone $\delta \leq -30^\circ$ have positive $v_{\rm LSR}$.

Members of the ensemble of compact, isolated HVCs will also be missed in spectral regions where substantial blending occurs due to foreground or background emission. Thus a CHVC with H I properties similar to those typical of the average listing in the table would remain undetected if the emission occurred blended with one of the major HVC complexes. Murphy, Lockman, & Savage (1995) estimate that some 18% of the sky is covered, at some velocities, by HVCs to the limit of the Hulsbosch & Wakker (1988) data. The major HVC complexes are responsible for such a high areal filling factor; the areal filling factor for the CHVCs tabulated here is very small.

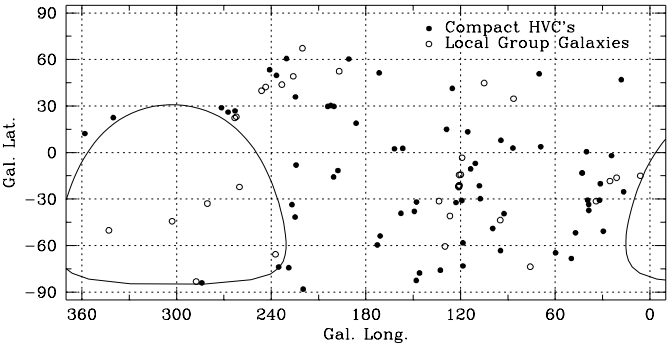

Fig. 2. Distribution on the sky of the compact, isolated HVCs, plotted as filled circles. The sample of CHVCs is unlikely to be complete, but it is, as discussed in the text, homogeneous and probably representative of this class of object. Unlike the major HVC complexes, the CHVCs are distributed rather uniformly over the sky. The sky distribution of Local Group galaxies (from Grebel 1997) is shown by open circles.

The matter of blending becomes more serious at the velocities spanned by the conventional gaseous disk of the Milky Way, because there the areal filling factor reaches 100%. Although all high–velocity clouds will have large space velocities, only the line–of–sight component of the motion is observed. An HVC could have a space velocity characteristic of the phenomenon, but an observed $v_{\rm LSR}$ of zero. Some known HVCs trespass on the kinematic regime of IVCs: for example, Complex C can be traced from the HVC regime into the kinematic regime associated with IVCs. The impressive spatial and kinematic continuities of the Magellanic Stream allow it to be followed as it traverses from highly deviant positive velocities to emerge at deviant negative velocities, even though it is lost due to blending as it crosses the kinematic regime of the conventional Milky Way gaseous disk, with radial velocities near zero.

But the additional information given by the spatial and kinematic continuities of a major HVC complex do not pertain for a compact HVC. If a CHVC were to emit near $v_{\rm LSR} = 0$ km s^{-1} (and if its total velocity width were not exceptionally large) then it will have gone unnoticed and will likely remain so. Thus deviation velocity is an incomplete discriminant, although a large deviation velocity is sufficient cause for considering an emission packet as an HVC, unless it can be separately demonstrated that emission is contributed from something else, e.g. from a galaxy. Blending thus limits the detection of compact HVCs to those with substantial deviation velocities. We comment further below on the possible consequences of this limitation.

We conclude that the principal causes for incompleteness of our sample are not systematic in the sense of discriminating against a particular portion of the sky, except for declinations less than -30° and, to a much lesser extent, $\delta < -18^\circ$, or in the sense of being kinematically incomplete, except for CHVCs which might have trespassed into the low–deviation regime at $|v_{\rm LSR}| < 50$ km/s. With these caveats, we view the sample as representative of the class of CHVC objects.

5. Discussion

We compare below the spatial and kinematic deployment of our CHVC sample with that of the galaxy members of the Local Group as compiled by Grebel (1997). The Local Group membership, as currently estimated, is certainly representative, even if there may be concerns with the completeness of the Local Group galaxy compilation somewhat analogous to those pertaining for the CHVC ensemble. It is not implausible that additional small galaxies of very low optical surface brightness will be found in the future; it is also not implausible that some Local Group galaxy, with brightness comparable to those already known, remains obscured by the Milky Way, either by dust extinction or by a high density of foreground stars. Another analogy may be drawn between the Local Group galaxy situation and the situation pertaining to the CHVCs, namely regarding the influence of the massive Local Group galaxies on the kinematics of objects lying near M31 or the Milky Way. The LMC, SMC, and the Sagittarius dwarf spheroidal, are in orbits dominated by the Milky Way, and M32 and other systems are in orbits dominated by M31, while other Local Group galaxies may be relatively isolated and distant from either M31 or the Milky Way, and may have experienced different evolutionary histories. If the CHVCs pervade the Local Group, a similar discrimination may pertain.

Fig. 2 shows the distribution on the sky of the compact, isolated HVCs, plotted as filled circles. The locations of galaxies comprising the Local Group (Grebel 1997) are plotted as open circles. The sky distribution of CHVCs shows a rather uniform deployment; in particular, CHVCs do not show the preference for the northern galactic hemisphere which the total–flux HVC distribution does, nor do the CHVCs show any tendency to cluster in streams or complexes.

Our primary concern, of course, is to seek information on the characteristic distance of the class of compact high–velocity clouds, as the values of most of the principal physical parameters depend on distance. The additional information which is available for a spatially resolved sample is not available here. Thus, Blitz et al. (1998) were able to use the angular size of extended, quite well resolved HVCs and HVC complexes to estimate distances in a statistical manner: nearer clouds would, on average, have a larger angular extent than more distant ones. Certain other important kinematic information is also lacking for our sample of generally unresolved sources, such as that pertaining to kinematic gradients across an extended feature due, for example, to rotation or to shearing. Little information is yet available which might reveal relevant details of the spatial structure of the CHVCs, except for the two entries, HVC 111−07−466 and HVC 114−10−430, for which Wakker & Schwarz (1991) obtained WSRT H I observations. It is striking that in both of those cases, the CHVCs are resolved into elliptical distributions of moderate column density embedded in diffuse envelopes of low column density. Each elliptical concentration shows a velocity gradient along the direction of maximum elongation, rather suggestive of rotation in a flattened disk system. Further H I interferometric observations of the CHVC phenomenon which might, for example, reveal a head–tail structure suggestive of passage through the halo of the Milky Way or through an intergalactic medium have not yet been obtained.

We note that because the CHVCs subtend such small angles it will be particularly difficult to find suitable probes for optical or UV absorption–line searches toward sources at known distances, thus possibly, in the most direct way, constraining, or even determining, the distance to a CHVC. It will similarly be particularly difficult to establish the metallicity of a CHVC.

As often done in astronomy, and certainly in H I work, we resort to the systemic velocities to support discussion of distances characteristic of the CHVC ensemble. Fig. 3 shows the kinematics of the ensemble of compact, isolated HVCs and of the ensemble of Local Group galaxies, plotted against galactic longitude for four different reference frames.

In the upper panel of Fig. 3, the longitude distribution of the motions of the CHVCs is shown, as filled circles, measured with respect to the Local Standard of Rest, as listed in column 8 of the table. Also plotted, as open circles, is the velocity/longitude distribution of the galaxies in the Local Group, from Grebel's (1997) catalog. It is appropriate to comment here on possible selection effects which might cause systematic distortions to the true distribution of CHVCs. The $\delta = -30^\circ$ declination limit of the LDS H I observations, as indicated in Fig. 2, is likely to have discriminated against some CHVCs at positive $v_{\rm LSR}$. This discrimination will remain in the other panels in Fig. 3, representing velocities in different reference frames. We might take the Small Magellanic Cloud as a test particle illustrative of the missing CHVCs, since it lies most central, of the Local Group galaxies, in the $\delta = -30^\circ$ oval plotted in Fig. 2. The SMC may be followed in the Fig. 3 panels, as the open circle near $l = 303^\circ$. Its velocity drops from +149 km/s in the $v_{\rm LSR}$ frame, to near zero velocity in the $v_{\rm GSR}$ and $v_{\rm LGSR}$ frames, and it is plausible to predict that not–yet–detected CHVCs would follow the same general tendency. There may further be a mild discrimination against detecting CHVCs due to their submersion in the "H I zone of avoidance", i.e. near $v_{\rm LSR} = 0$ km s^{-1}, with the velocity distribution slightly skewed to negative $v_{\rm LSR}$ in galactic quadrant II, and slightly skewed to positive velocities in quadrant III.

In the second panel from the top of Fig. 3, the motions of the CHVC ensemble and of the Local Group galaxies are plotted with respect to the Galactic Standard of Rest; and in the third panel, with respect to the Local Group Standard of Rest. The adopted definitions of the various velocity systems with units of km s^{-1} are:

$$\begin{aligned} v_{\rm LSR} &= v_{\rm HEL} + 9\cos(l)\cos(b) \\ &\quad +12\sin(l)\cos(b) - 7\sin(b) \qquad (1) \\ v_{\rm GSR} &= v_{\rm LSR} + 0\cos(l)\cos(b) \\ &\quad +220\sin(l)\cos(b) + 0\sin(b) \qquad (2) \\ v_{\rm LGSR} &= v_{\rm GSR} - 62\cos(l)\cos(b) \\ &\quad +40\sin(l)\cos(b) - 35\sin(b) \qquad (3) \end{aligned}$$

Fig. 4 shows histograms of the velocities in these reference frames; the dispersion of the velocities decreases in a progres-

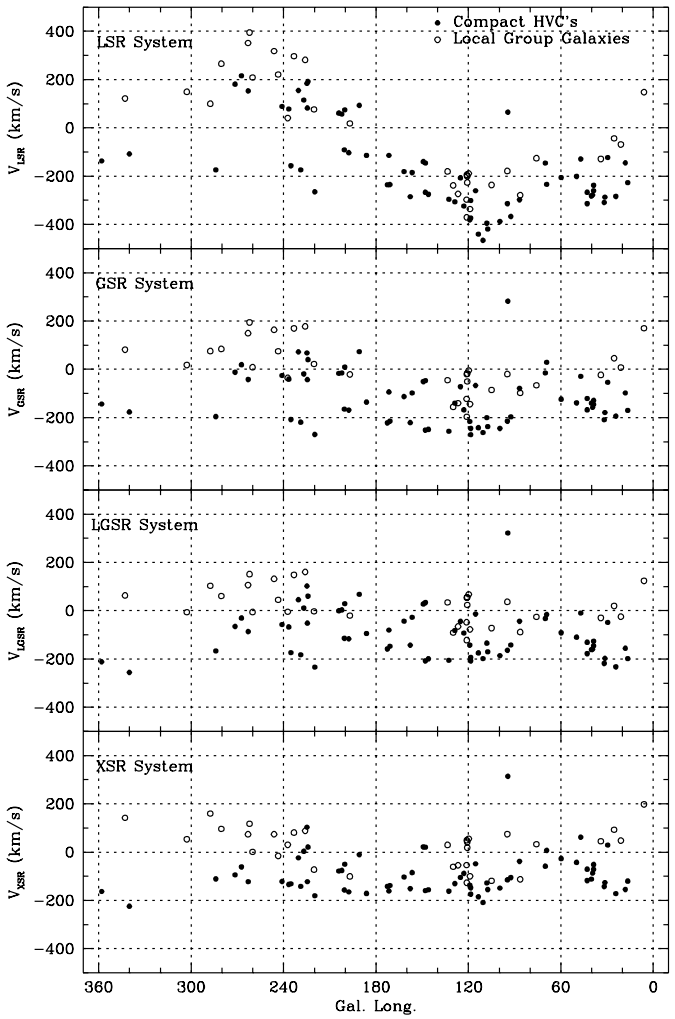

Fig. 3. Velocities of the ensemble of compact, isolated HVCs and of the ensemble of Local Group galaxies, plotted against galactic longitude for four different kinematic reference frames. The CHVCs are shown as filled circles; the members of the Local Group, as open circles. In the upper panel, the motions of the CHVCs are shown measured with respect to the Local Standard of Rest; in the second panel from the top, with respect to the Galactic Standard of Rest; and in the third panel, with respect to the Local Group Standard of Rest. Fig. 4 shows histograms of the velocities in these reference frames; the dispersion of the velocities decreases in a progression from the $v_{\rm LSR}$ reference frame, via the $v_{\rm GSR}$ one, to the $v_{\rm LGSR}$ frame. The bottom panel here shows the CHVC motions measured with respect to a reference frame, labeled XSR, which minimizes the dispersion of the motions.

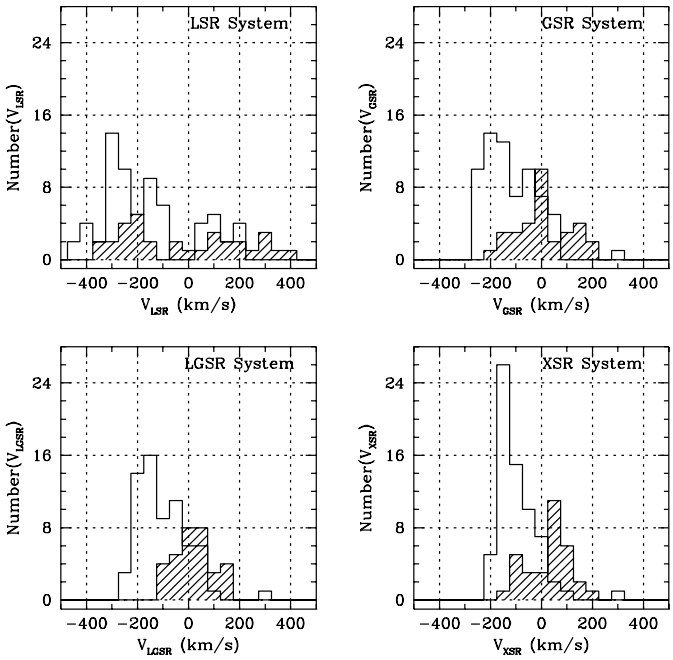

Fig. 4. Histograms of distributions of the CHVC velocities, and of Local Group galaxy velocities, as measured in the reference frames indicated on the abscissæ. The open histograms represent the CHVC ensemble; the hatched histograms, the Local Group galaxies. The dispersion of the histogram representing the $v_{\rm LGSR}$ frame is significantly smaller than that in the $v_{\rm LSR}$ and $v_{\rm GSR}$ reference frames. The velocities labelled $v_{\rm XSR}$ refer to a frame which was found to minimize the dispersion of the CHVC velocity distribution.

sion from the $v_{\rm LSR}$ reference frame, for which $\sigma_{\rm LSR} = 175$ km s^{-1}, via the $v_{\rm GSR}$ one ($\sigma_{\rm GSR} = 95$ km s^{-1}), to the $v_{\rm LGSR}$ frame, for which $\sigma_{\rm LGSR} = 88$ km s^{-1}. As noted by Blitz et al. (1998) a decreasing velocity dispersion for a population gives a good indication that a more appropriate reference frame is being approached. They cite the example of the globular cluster system of the Galaxy, for which the velocity dispersion drops from 134 to 119 km s^{-1} in going from the LSR to the more relevant GSR frame.

Since our CHVC sample has both a substantial size and an essentially uniform distribution on the sky (Fig. 2) it is appropriate to use the sample itself to define a best-fitting velocity reference system. We have determined the direction cosine coefficients that provide a minimum velocity dispersion of the measured radial velocities. The result of this optimization has been labeled the "XSR system" and is defined by:

$$\begin{aligned} v_{\rm XSR} &= v_{\rm GSR} + 0\cos(l)\cos(b) \\ &\quad +45\sin(l)\cos(b) - 90\sin(b) \end{aligned} \tag{4}$$

The velocity dispersion of the CHVC sample in the XSR system is only $\sigma_{\rm XSR} = 69$ km s^{-1}. The accuracy of the coefficients of the direction cosines, and therefore the implied solar apex $(l_\odot, b_\odot, v_\odot) = (88°, -19°, +293$ km s$^{-1})$, is, however, not very high. Varying each coefficient by plus and minus 50 km s^{-1} increases the dispersion of the distribution from its minimum value to about 75 km s^{-1}. Comparable uncertainties of perhaps 50 km s^{-1} also apply to the coefficients which define the LGSR frame, $(l_\odot, b_\odot, v_\odot) = (93°, -4°, +316$ km s$^{-1})$ according to Karachentsev & Makarov (1996), implying agreement between these two frames at about the one sigma level. This is particularly interesting since the XSR system was defined completely independently on the basis of the CHVC system alone.

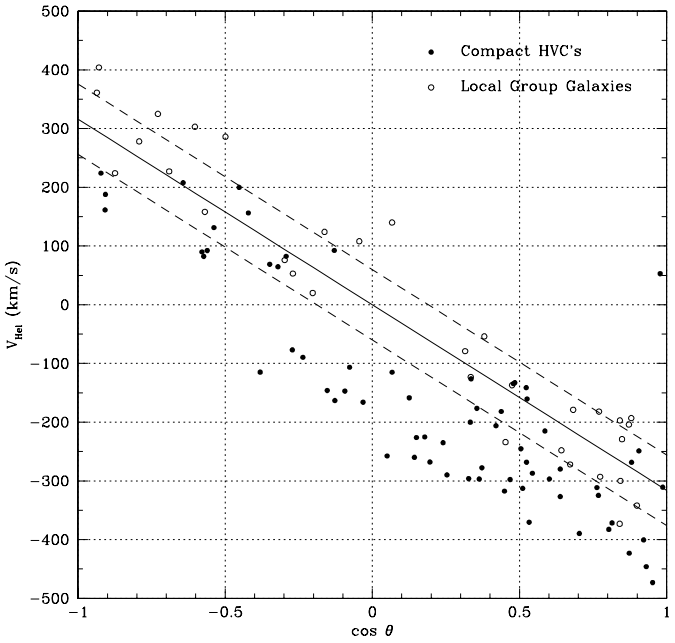

Fig. 5. Variation of heliocentric velocity versus the cosine of the angular distance between the solar apex and the (l, b) direction of the object. Members of the compact, isolated high–velocity cloud ensemble are plotted as filled circles; galaxies comprising the Local Group, as open circles. The solid line represents the solar motion of $v_\odot = 316$ km s^{-1} toward $l = 93°$, $b = -4°$ as determined by Karachentsev & Makarov (1996) and used by Grebel (1997) in her analysis. The dashed lines represent the $\sigma(v)$ envelope, one standard deviation (± 60 km s^{-1}, following Sandage 1986) about the velocity/angular–distance relation, pertaining for galaxies considered firmly established as members of the Local Group.

Fig. 5 shows the heliocentric velocity plotted against the cosine of the angle between the solar apex and the direction to the CHVCs, indicated by closed circles, and the directions to the Local Group galaxies, indicated by open circles. Such displays of the kinematics have been used to ascertain membership of galaxies in the Local Group by Sandage (1986), van den Bergh (1994), Grebel (1997), and others. The dashed lines at ± 60 km s^{-1} represent the 1–σ envelope considered by Sandage (1986) to describe the dispersion of the Local Group membership. Van den Bergh (1994) notes that galaxies on the outer fringe of the Local Group, about 1 Mpc distant from the Local Group barycenter, tend to lie above the upper envelope. Galaxies with quite large positive–velocity deviations would be partaking in the cosmological expansion, and at distances substantially greater than 1 Mpc. We note that the filled circle most deviant from the mean of the CHVC objects is the galaxy interloper, Cepheus 1, which Burton et al. (1999) judge, mainly by its angular and kinematic proximity to NGC 6946, to be at a distance of approximately 6 Mpc. The most deviant of the Local Group galaxies is the Sagittarius dwarf spheroidal, which lies so close to the Milky Way that its motion would be gravitationally distorted and thus not representative of the Local Group ensemble. The position of Cepheus 1 ($l = 94°$) and of the Sagittarius dwarf spheroidal ($l = 6°$) are also, not surprisingly, unrepresentative of the means in the velocity/longitude plots of Fig. 3.

Despite the similarities between the deployment of the CHVCs and the Local Group galaxies in Figs. 3 and 5, there is a clear tendency for the distribution of CHVC velocities to have a negative mean. This same tendency is evident at most galactic longitudes and in all reference frames, but is of course clearest in the LGSR and XSR frames for which a net infall of the CHVCs with a mean velocity of about 100 km s^{-1} is measured. This point needs some further investigation in terms of the selection criteria of the CHVC sample, in particular to gauge the extent to which undetected CHVCs with $v_{\rm LSR}$ near zero might influence the result. Inspection of the LSR velocity histogram in Fig. 4 suggests that perhaps a total of 8 objects might be missing in this velocity range from an otherwise continuous distribution. It seems unlikely that inclusion of the "missing" objects would dramatically influence the result. Taken at face value, these kinematics are suggestive of a population which is bound to the Local Group, but which has not yet experienced significant interaction or merger with the larger members, which would tend to virialize their motions. A mean radial infall velocity which is comparable to the velocity dispersion of the Local Group member galaxies, $\sigma_{\rm LGSR} = 76$ km s^{-1}, is quite plausible if the same gravitational potential is responsible for both. Perhaps of relevance is the fact that Côté et al. (1997) found that the faint dwarf galaxies in the two groups of galaxies nearest to the Local Group show a wider range of velocity distribution than the brighter members. An evolutionary history which is a function of mass may be a natural part of the galaxy formation process.

6. Summary

We have attempted to determine an objectively defined class of high–velocity clouds, which might represent a homogeneous subsample of these objects, in a single physical state. The selection criteria led to a catalog of compact, isolated high–velocity clouds; the criteria excluded the Magellanic Stream and all of the other known HVC complexes from our considerations. We are, of course, aware that the total H I flux represented by all of the CHVCs is less than that from a single large complex. A full explanation of the HVC phenomenon will have to subsume the complexes as well as the compact objects, and it is not yet clear if a single, unifying explanation will suffice.

No direct distance determination is yet available for any of the objects. Several aspects of the topology of the class are difficult to account for if the CHVCs are viewed as a Milky Way population, in particular if they are viewed as consequences of a galactic fountain. The amplitude of the horizontal motions of these "bullets" is comparable to that of the vertical motions. The vertical motions are larger than expected for free fall onto the Milky Way from material returning in a fountain flow. There is no preference shown for the terminal–velocity locus, where motions from violent events leading to a fountain would be expected to be most common. Unlike the situation if the major HVC complexes are considered, the CHVCs

are scattered rather uniformly across the sky, with no strong preference for the northern galactic hemisphere. The CHVCs show no tendency to accumulate in the lower halo of the Milky Way. The CHVCs also show no tendency to cluster along filamentary structures. Regarding both their spatial and kinematic distributions, the CHVCs show substantial similarities with the distributions of the galaxies comprising the Local Group. The solar apex which follows directly from a minimization of the velocity dispersion of the CHVC system namely, $(l_\odot, b_\odot, v_\odot) = (88°, -19°, +293 \text{ km s}^{-1})$, agrees within the errors with that which defines the Local Group Standard of Rest, $(l_\odot, b_\odot, v_\odot) = (93°, -4°, +316 \text{ km s}^{-1})$, found by Karachentsev & Makarov (1996). The velocity dispersion of the CHVC system in this reference frame is only $\sigma_{\rm XSR} = 69 \text{ km s}^{-1}$, while there is a mean infall of $v_{\rm LGSR} = v_{\rm XSR} = -100 \text{ km s}^{-1}$.

It seems that the most plausible reference system for the CHVC deployment and kinematics is that of the Local Group. The low velocity dispersion in this reference frame and substantial radial infall are strongly suggestive of a population which has as yet had little interaction with the more massive Local Group members, which have both a slightly larger velocity dispersion $\sigma_{\rm LGSR} = 76 \text{ km s}^{-1}$ and a small positive mean velocity $v_{\rm LGSR} = +22 \text{ km s}^{-1}$. At a typical distance of about 1 Mpc the CHVCs would have sizes of about 15 kpc and gas masses, $\rm M_{HI}$, of a few times $10^7 \rm M_\odot$, corresponding to those of (sub-)dwarf galaxies. Although the total gas mass represented by our entire sample would not be large, $\rm M_{HI}$, of a few times $10^9 \rm M_\odot$, it is still quite substantial. More importantly, the CHVCs may still represent pristine examples of collapsed objects, with only a small amount of internal star formation and enrichment. As such, they should provide substantial insight into the process of galaxy and structure formation.

Since the inception of high–velocity cloud research, the possibility of an extragalactic deployment of these clouds has been critically considered as a possibility; among others, the discussions by Oort (1966, 1970, 1981), Verschuur (1975), Giovanelli (1981), Bajaja, Morras, & Pöppel (1987), Wakker & van Woerden (1997), and Blitz et al. (1998) are particularly relevant here. The role played by the HVC complexes is important to each of these discussions. Giovanelli (1981) tried, as we have done here, to define an appropriately unambiguous subsample of HVCs, which avoided the complexes: his subsample of HVCs with extreme (negative) velocities lay in one galactic quadrant, at $l < 180°$ and $b < 0°$. Giovanelli considered it more likely that the HVCs in his sample were shreds of the Magellanic Stream precipitating toward the galactic disk. We note that the sample of CHVCs considered here covers much of the sky, and includes members far removed in both angle and velocity from the Magellanic Stream; we note also that the Local Group galaxies with the most extreme (negative) velocities – see Fig. 3 – also populate that single quadrant. Blitz et al. (1998), who also remove the Magellanic Stream and several major complexes from their discussion, justify this distinction as not arbitrary, but supported by observational constraints on the distances of the excluded complexes. They conclude that the remaining HVC material, including a substantial flux residing in the remaining complexes, is falling onto the Local Group. Blitz et al. connect the HVC properties to the hierarchical structure formation scenario, and to the gas seen as Lyman–limit clouds in absorption towards quasars; some of their predictions and considerations are also relevant for the CHVCs.

Several aspects of the compact, isolated high–velocity objects seem particularly appropriate for further observations. Many of the CHVCs cataloged are suitable candidates for H I radio interferometry. The CHVCs show such a wide range of observed linewidths that a number of questions arise concerning stability and possible rotation. It would be interesting to see if any of the CHVCs showed internal kinematics, particularly rotation, at an amplitude which would indicate the presence of dark matter, or which might suggest that the objects resemble dwarf galaxies in which stars have not yet been found, or have simply not formed. Although it seems that optical or UV absorption–line studies will be hindered by a paucity of suitable background probes, many of the CHVCs are suitable candidates for deep probes of optical emission. If the CHVCs are at Local Group distances, the diffuse Hα emission surrounding the CHVCs would be less bright than that associated with the HVCs in complexes lying in the halo of the Milky Way. However, the Hα emission from even a single H II region or Planetary Nebula could be easily detected, and this would allow immediate recognition of an associated stellar population and hence a distance. Deep optical probes would help clarify the distinction between the CHVCs and nearby dwarf galaxies, and would, at least, reveal any remaining major interloper like Cepheus 1 which we found masquerading in our catalog as HVC 094+08+080.

Acknowledgements. We are grateful to B. P. Wakker for providing us with a digital version of the (updated) HVC catalogue of Wakker & van Woerden (1991), and to E. K. Grebel for providing a digital version of her catalogue of members of the Local Group. The Dwingeloo radio telescope is operated by the Netherlands Foundation for Research in Astronomy, under contract with the Netherlands Organization for Scientific Research. The Green Bank 140–foot telescope is operated by the National Radio Astronomy Observatory under contract with the U. S. National Science Foundation; we are grateful to F. J. Lockman and D. Balser for obtaining some of the Green Bank spectra at our request.

References

Bajaja E., Cappa de Nicolau C.E., Cersosimo J.C., et al., 1985, ApJS 58, 143

Bajaja E., Morras R., Pöppel W.G.L., 1987, Pub. Astr. Inst. Czech. Ac. Sci. 69, 237

Blitz L., Spergel D.N., Teuben P.J., Hartmann D., Burton W.B., 1998, ApJ, submitted

Bregman J.N., 1980, ApJ 236, 577

Burton W.B., 1997, In: Lesch H., Dettmann R.-J., Mebold U., Schlickeiser R. (eds.) The Physics of the Galactic Halo. Akademie Verlag, Berlin, 15

Burton W.B., Braun R., Walterbos R.A.M., Hoopes C.G., 1999, AJ, in press

Cohen R.J., Mirabel I.F., 1979, MNRAS 186, 217

Côté S., Freeman K.C., Carignan C., Quinn P.J., 1997, AJ 114, 1313

Danly L., Albert C.E., Kuntz K.D., 1993, ApJ 416, L29

Davies R.D., 1975, MNRAS 170, 45P
Einasto J., Lynden-Bell D., 1982, MNRAS 199, 67
Giovanelli R., 1981, AJ 86, 1468
Giovanelli R., Haynes M.P., 1977, A&A 54, 909
Grebel E.K., 1997, Star Formation Histories of Local Group Dwarf Galaxies. Reviews in Modern Astronomy 10, 29
Hartmann D., 1994, Ph.D. Thesis, University of Leiden
Hartmann D., Kalberla P.M.W., Burton W.B., Mebold U., 1995, A&AS 119, 115
Hartmann D., Burton W.B., 1997, Atlas of Galactic Neutral Hydrogen. Cambridge University Press
Henning P.A., 1992, ApJS 78, 365
Hulsbosch A.N.M., 1978, A&A 66, L5
Hulsbosch A.N.M., Wakker B.P., 1988, A&AS 75, 191
Karachentsev I.D., Makarov D.A., 1996, AJ 111, 794
Mathewson D.S., Cleary M.N., Murray J.D., 1974, ApJ 190, 291
Mirabel I.F., 1981, ApJ 247, 97
Mirabel I.F., Cohen R.J., 1979, MNRAS 188, 219
Muller C.A., Oort J.H., Raimond E., 1963, C.R.Acad.Sci.Paris 257, 1661
Murphy E.M., Lockman F.J., Savage B.D., 1995, ApJ 447, 642
Oort J.H., 1966, Bull. Astr. Inst. Netherlands 18, 421
Oort J.H., 1970, A&A 7, 381
Oort J.H., 1981, A&A 94, 359
Reynolds R.J., Tufte S.L., Haffner L.M., Jaehnig K., Percival J.W., 1998, PASA 15, 14
Sandage A., 1986, ApJ 307, 1
Shapiro P.R., Field G.B., 1976, ApJ 205, 762
van den Bergh S., 1994, AJ 107, 1328
van Woerden H., Wakker B.P., Schwarz U.J., Peletier R., Kalberla P.M.W., 1998, In: Breitschwerdt D., Freyberg M.J., Trümper J. (eds.) IAU Coll. 166, The Local Bubble and Beyond. Lecture Notes in Physics 506, 467
Verschuur G.L., 1975, ARA&A 13, 257
Wakker B.P., 1991, A&A 250, 499
Wakker B.P., Schwarz U., 1991, A&A 250, 484
Wakker B.P., van Woerden H., 1991, A&A 250, 509
Wakker B.P., van Woerden H., 1997, ARA&A 35, 217
Williams, D.R.W., 1973, A&AS 8, 505
Wright M.C.H., 1979, ApJ 233, 35